Phase-Change Materials

International Edition: DOI: 10.1002/anie.201501032
German Edition: DOI: 10.1002/ange.201501032

Extensively Reversible Thermal Transformations of a Bistable, Fluorescence-Switchable Molecular Solid: Entry into Functional Molecular Phase-Change Materials**

*P. Srujana and T. P. Radhakrishnan**

Abstract: *Functional phase-change materials (PCMs) are conspicuously absent among molecular materials in which the various attributes of inorganic solids have been realized. While organic PCMs are primarily limited to thermal storage systems, the amorphous–crystalline transformation of materials like Ge-Sb-Te find use in advanced applications such as information storage. Reversible amorphous–crystalline transformations in molecular solids require a subtle balance between robust supramolecular assembly and flexible structural elements. We report novel diaminodicyanoquinodimethanes that achieve this transformation by interlinked helical assemblies coupled with conformationally flexible alkoxyalkyl chains. They exhibit highly reversible thermal transformations between bistable (crystalline/amorphous) forms, along with a prominent switching of the fluorescence emission energy and intensity.*

Materials that can exist in reversibly interconvertible phases, with a substantial transition enthalpy or switching of a property between the phases, are known as phase-change materials (PCMs).[1] The common organic PCMs such as paraffins, fatty acids/alcohols/esters, and polymers are primarily used in energy-storage applications (the latent heat associated with the solid–liquid transition used for energy storage/release),[2–4] and occasionally in drug delivery vehicles.[5,6] Inorganic PCMs include salt hydrates used in thermal storage systems,[7,8] and compounds like $Ge_2Sb_2Te_5$ (GST) that find unique applications in information storage owing to the efficient switching between the crystalline and amorphous phases possessing significantly different optical reflectivity and electrical conductivity.[9–11] The amorphous–crystalline PCMs are of special interest owing to the all-solid-state nature and the small volume/strain changes across the phase boundary; the bistability is critical for device applications. Compared to inorganic materials, small molecule-based organic solids are advantageous owing to their tailorable fabrication by soft chemistry and lower operating temperatures. The unique optical, magnetic, or electronic responses of functional molecular materials can considerably expand the scope of PCMs.

Most of the properties observed in inorganic solids have been realized in molecular materials over the last several decades,[12] and the relevance of the amorphous state in molecule-based materials[13] and pharmaceuticals[14] has been established; however, no PCM has been developed using functional molecular materials. Bistable amorphous-crystalline PCMs of any kind, organic or inorganic, capable of thermally induced, multiple, reversible switching of sensitive optical attributes such as fluorescence emission are unknown. The closest that we are aware of are hybrid systems in which the luminescence of a semiconductor quantum dot or a conjugated polymer is switched indirectly through phase changes of an overlayer of GST or paraffin wax deposited in situ, respectively.[15,16] Fluorescence switching in molecular systems have been achieved by photoactivated reactions[17] and thermochromism.[18] Fluorescence change upon crystal-to-crystal transformation[19] and formation of partially amorphous states upon grinding[20] with limited cycling have been reported. In none of the cases was either a well-characterized amorphous phase and bistability established, or extensive amorphous–crystalline cycling exclusively by thermal processing demonstrated. Even though reversible thermal transformations of an anthraquinone derivative accompanied by a circa 20% variation in the reflectivity was reported, the phases (amorphous/crystalline) were not clearly characterized, and more significantly, there is no switching of functional attributes like fluorescence emission.[21]

Molecular materials based on the diaminodicyanoquinodimethane (DADQ) system[22] that produce strong optical second harmonic generation[12,23] as well as enhanced fluorescence in the solid state[24] have been developed in our laboratory. Recently, amorphous nanoparticles of a DADQ derivative were fabricated and transformed to the crystalline state with different fluorescence emission, by solvent vapor fuming.[25] However, reversible transformation, preferably thermally induced, is required to realize a viable PCM. Most of the DADQs possess melting temperatures near 250 °C and decompose during melting, preempting the possibility of realizing an amorphous state or reversible transformations; decomposition during melting is indeed, a problem with many functional organic molecule-based materials. Exploration with a variety of substituent groups has now led to the synthesis of novel derivatives of DADQ (Figure 1 a) that melt at lower temperatures ($T_m \approx 150$ °C) with no decomposition. Quenching the melts produces amorphous materials at

[*] P. Srujana, Prof. T. P. Radhakrishnan
School of Chemistry, University of Hyderabad
Hyderabad—500 046 (India)
E-mail: tpr@uohyd.ac.in
Homepage: http://chemistry.uohyd.ac.in/~tpr/

[**] Financial support from the DST and the UGC, New Delhi and infrastructure support from the Central Facility for Nanotechnology and the School of Chemistry, University of Hyderabad are acknowledged with gratitude. We thank Ms. Nalini for help with the confocal fluorescence microscopy measurements. P.S. thanks the CSIR, New Delhi for a Junior Research Fellowship.

Supporting information for this article is available on the WWW under http://dx.doi.org/10.1002/anie.201501032.

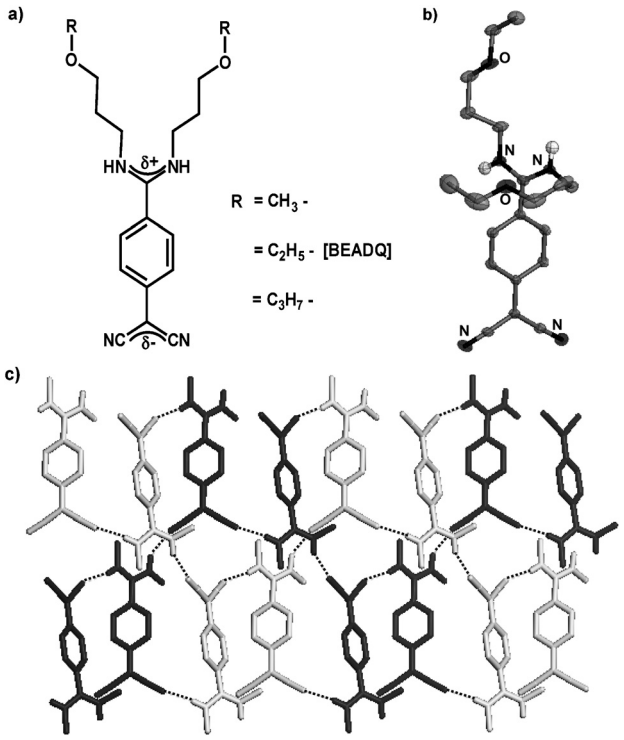

Figure 1. a) Structure of the new DADQs. b) Molecular structure of BEADQ from single crystal analysis. Ellipsoids are set at 90% probability; C gray, H white; N, O are indicated with labels and all H atoms except those in amino groups involved in the H-bonds are omitted for clarity. c) The intertwined and linked helical assemblies of molecules in the crystal lattice of BEADQ, formed through intermolecular H-bonds (broken lines); molecules in the two chains are shown in black and white.

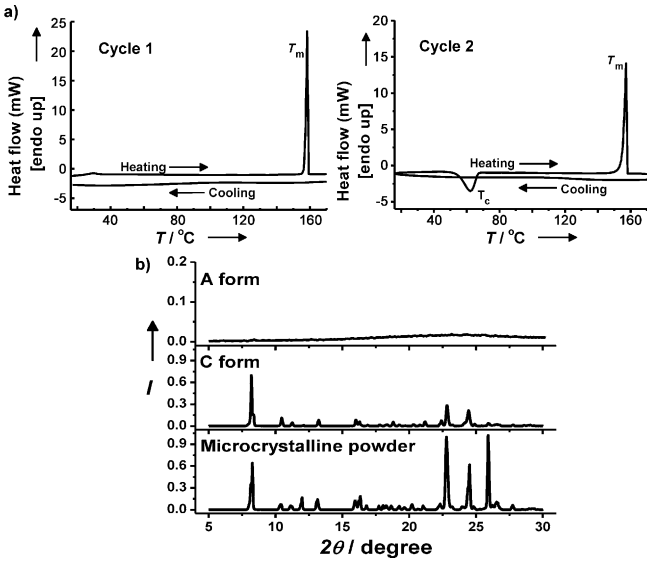

Figure 2. a) Differential scanning calorimetry thermograms of solid BEADQ through two heating (2 °C min^{-1})–cooling (20 °C min^{-1}) cycles; the melting (T_m) and crystallization (T_c) temperatures are indicated. b) X-ray diffraction pattern of the microcrystalline powder and the **C** and **A** forms.

ambient temperatures, which can then be transformed back to the crystalline state by heating to temperatures (T_c) of about 70 °C and cooling slowly; this reversible transformation can be repeated several times. Most significantly, the bistable amorphous/crystalline forms exhibit strikingly different fluorescence emission responses, in terms of intensity (weak/strong) as well as color (cyan/blue). The representative molecule, 7,7-bis(ethoxypropylamino)-8,8-dicyanoquinodimethane (BEADQ) is described in detail herein; salient observations with the other derivatives are provided in the Supporting Information.[26]

BEADQ was synthesized by the direct single-step reaction of 3-ethoxypropylamine with TCNQ in acetonitrile.[26] The molecular structure and assembly in crystals[27] are shown in Figure 1 b,c. The molecule has the zwitterionic structure typical of DADQs,[23,28] with a dihedral twist angle (θ) of about 46.7° between the diaminomethylene moiety and the benzenoid ring. The conformationally flexible alkoxyalkyl chains are the crucial structural elements that can induce disorder in the lattice and disturb the packing of the DADQ framework under suitable conditions. Molecular assembly in the crystal involves intertwining, linked helical superstructures of H-bonded molecules (Figure 1 c); the extended supramolecular interactions are likely to help in regaining the integrity of ordered assemblies from the amorphous state. DSC thermograms of BEADQ are collected in Figure 2 a. In the first heating run carried out at a slow rate of 2° min^{-1}, the microcrystalline sample melts at 158 °C (T_m); a fast cooling reveals no crystallization event. Heating in the second cycle shows an exothermic peak at 65 °C; this corresponds to the crystallization temperature (T_c), as the endothermic peak that is due to the melting reappears at 156–157 °C. The melt–quench–recrystallize cycle can be repeated several times with high reproducibility, confirming the reversibility of the transformations. The slight depression in the T_m with respect to that in the first cycle occurs consistently in the repeat cycles. The enthalpy change associated with the melting and crystallization transitions (ca. 74–82 J g^{-1})[26] are smaller than that of the melting of organic PCMs used in energy storage (ca. 100–300 J g^{-1}).[29] The T_c was found to increase from 65 °C to 83 °C when the heating rate was varied from 2° min^{-1} to 16° min^{-1} [26] indicating the relevance of kinetic effects in the recrystallization. The powder X-ray diffraction patterns (Figure 2 b) confirm the amorphous and crystalline state of the melt-quench (A form) and recrystallized (C form, the melt-quench form heated at 70 °C for 10 min and cooled) samples respectively; the former shows no clear diffraction peaks whereas the latter agrees fully with the pattern of the original microcrystalline sample, which in turn can be simulated using the crystal structure of BEADQ.[26]

Several procedures were explored to prepare BEADQ in the A and C forms to carry out spectroscopy/microscopy investigations and realize multiple interconversions. Form A was found to convert into C fairly quickly in bulk powder samples. On the other hand, thin films prepared on different substrates by drop-casting the solution as well as by covering a drop-cast film with a thin polymer over-layer, tended to stabilize A, making the conversion into C difficult; similar was the experience with spin-cast polymer films doped with the compound. Finally it was found that thin film samples

sandwiched between 0.15 mm thick glass cover slips when melted and quenched, produced stable A form; when maintained at the laboratory temperature of 25 °C, the fluorescence emission signature (discussed below) was fully reproducible for several hours. Form A could be converted into stable C by heating at 70 °C for 10 min.

Electronic absorption spectra of BEADQ in solution, microcrystalline solid and the A and C forms are collected in Figure 3a; the inset shows the photographs of the latter. Broadening of the absorption spectra of the solids arises owing to the intermolecular interactions; the relatively higher broadening in A points to the disordered environment of the chromophores. To understand the influence of molecular interactions on the optical spectra of the crystals and thin films,[25,30] we have computed the electronic excitation energies of BEADQ molecule in different environments, using ab initio TD-DFT calculations at the B3LYP/6-31G* level.[26] Table 1 shows the good agreement between the λ_{max} computed for the lowest energy excitation having appreciable oscillator strength, and the relevant experimental observations; in the case of the solids, the experimental value corresponds to the approximate midpoint of the broad peak. Polar solvents shift the absorption to higher energy with respect to that of the molecule in vacuum, which is due to the stabilization of the strongly zwitterionic ground electronic state; this solvatochromic effect is adequately modeled by inclusion of the solvent in the computation.[26] The simplest approach to model the impact of the local field owing to the neighboring molecules in the solid state of the DADQ molecule is to introduce positive and negative point charges at the positions of the diaminomethylene and dicyanomethylene carbon atoms respectively, of the closest neighbors in the crystal lattice, representing the major dipole corresponding to the zwitterionic structure. The magnitude of the charge, 0.83 *e*, was estimated from the computed dipole moment of the BEADQ molecule and the distance between these carbon atoms.[26] The λ_{max} value estimated with the imposition of such a local field around BEADQ agrees very well with the experimental observation on the microcrystalline solid and the C form. The physical basis for the blue-shift of the absorption with respect to that of the isolated molecule is the enhancement of the intramolecular charge transfer energy owing to the opposing field of near neighbor dipoles. Moving the dipoles away from the BEADQ molecule increases the λ_{max}, explaining the red-shift of the absorption in the A form.

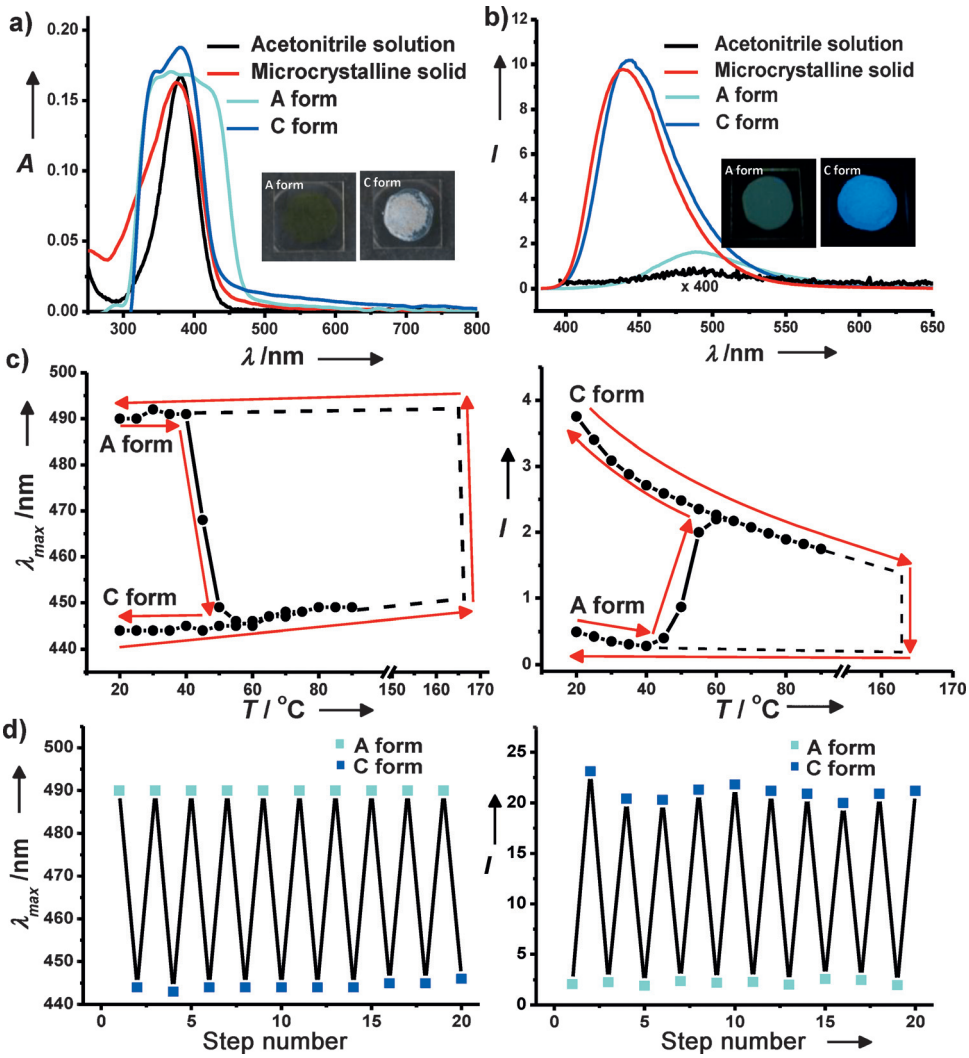

Figure 3. a) Absorption spectra of acetonitrile solution, microcrystalline solid, melt-quench (A) and recrystallized (C) forms of BEADQ (inset: optical images of the latter two under ambient light). b) Fluorescence emission spectra of acetonitrile solution, microcrystalline solid, melt-quench (A) and recrystallized (C) forms of BEADQ, with λ_{exc} = 380 nm (solution) and 368 nm (others); relative intensities of the samples with similar optical density are shown; the solution spectrum is multiplied by a factor of 400 (inset: optical images of the latter two under 365 nm light). c) Plots of the fluorescence emission peak wavelength and intensity during the transformation of the A to the C form; the broken line shows a representation of the reverse transformation. d) Repeated switching of the fluorescence emission wavelength and peak intensity associated with the reversible A⇄C transformations of BEADQ.

The fluorescence emission spectra of BEADQ in solution, microcrystalline solid, and the A and C forms are collected in Figure 3b; the inset shows the photographs of the latter under 365 nm (UV) light. Molecule in the A

Table 1: The lowest-energy electronic absorption peak maxima (λ_{max}) for BEADQ in different experimental conditions and the values computed by TD-DFT method at B3LYP/6-31G* level, using different environments.[a]

Experiment		Computation		
State of BEADQ	λ_{max} [nm]	λ_{max} [nm]	Molecular geometry	Molecular environment
–	–	460.3	from crystal[b]	vacuum
acetonitrile solution	384	385.6	optimized[c]	acetonitrile
microcrystalline solid	377	376.2	from crystal[b]	field of dipoles
C form	374			(as in crystal)
A form	390	391.7	from crystal[b]	field of dipoles (moved away)

[a] Environments: in vacuum, in acetonitrile using the SCRF model, and with a field of five nearest-neighbor dipoles kept at distances as in the crystal lattice as well as moved away from their positions by 9%. [b] Average dihedral angle, $\theta = 46.7°$. [c] Fully optimized with acetonitrile solvent; average $\theta = 37.2°$.

form with a disordered structure resembles the solvated individual molecule in solution as seen from the similarity with the solution spectrum. The spectra show a distinct shift in the emission peak from 444 nm in C to 489 nm in A, reflecting the shift in the absorption. The emission intensity of A is approximately an order of magnitude lower than that of C; the quantum yields measured are 3.5% and 40%, respectively (the quantum yield of the solution and microcrystalline solid are 0.1% and 48%, respectively). Steady enhancement in the fluorescence emission from the solution, to the A form, and then to the C and microcrystalline forms, can be attributed to the increasing rigidification of the molecular environment and the consequent reduction in the torsional relaxation of the electronic excited state, which otherwise provides a non-radiative pathway for the excited state energy loss.[24] Plots of the peak wavelength and intensity of the fluorescence emission accompanying the thermal transformation of the A to the C form (Figure 3c) demonstrates clearly the bistability of the system; the reverse transformation is shown schematically. Figure 3d shows the switching of the fluorescence emission wavelength as well as intensity of samples at ambient temperature, through repeated A⇄C conversions. The regularity and uniformity of the switching demonstrates the new, extensively reversible functional PCM based on a molecular material; it is important to note that the cycling is induced by easily accessible thermal conditions. As the transmittance also changes between the C and A forms, its switching (ca. 30–100%) can also be monitored through repeated cycles.[26] The fluorescence variation in terms of energy and intensity is indeed more sensitive than the changes in polarized light transmittance observed between crystalline and amorphous forms.

Laser scanning confocal fluorescence microscope images of the A and C forms (Figure 4a) show that, while the former is a smooth film, the latter has a polycrystalline morphology. Overlap of the spectral responses recorded in the microscope (Figure 4b) shows that only the C form emits in the 400–430 nm window. Images of A samples heated at 70°C for 1–9 min, recorded using the emission in this narrow range (Figure 4c) reveals graphically the formation and growth of the crystalline domains in the thin film. Similar observations can also be made with A samples heated for 1 min at temperatures ranging from 60–100°C, the spectral response shifting smoothly from that of the A form to the C form.[26] Polarization dependence of the fluorescence spectra indicates no anisotropy in the A form, but a small value in the case of the C form.[26] Raman spectra of the microcrystalline powder and C and A forms of BEADQ recorded in a confocal Raman microscope are collected in Figure 5. Spectrum of the C form clearly matches that of the microcrystalline material; as is often found,[31] the spectrum of the A form has relatively broader peaks and background. Even though the C and A forms show many common bands, some are conspicuously absent and a few split bands merge in the A form. This effect could be due to the soft phonon (intermolecular) or librational modes, or split-degeneracies which arise only in the crystalline structure. Possibility of some of the modes that are sensitive to the conformation of the alkoxyalkyl chains

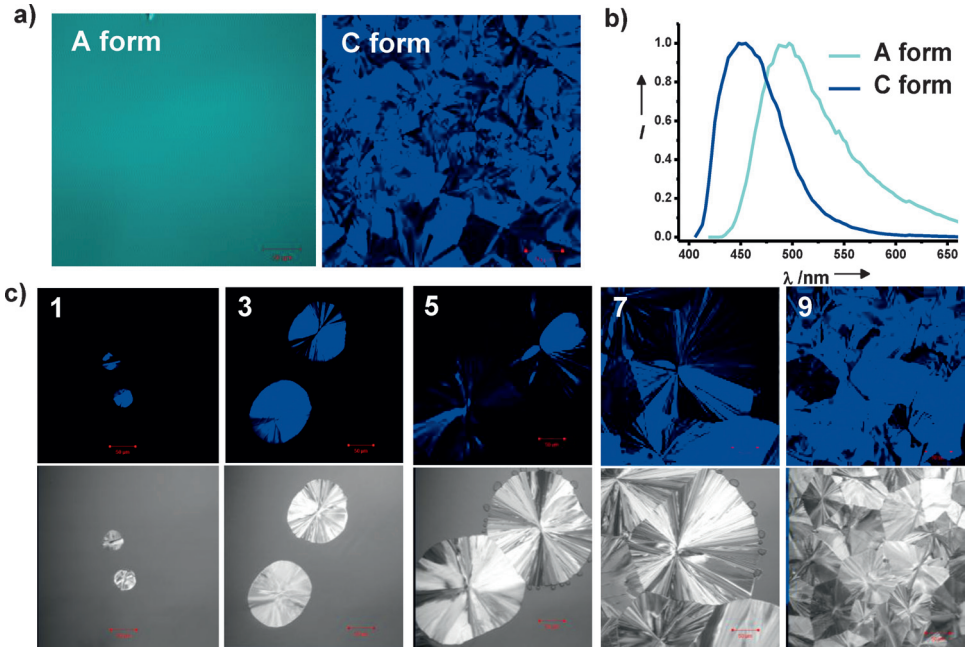

Figure 4. a) Images and b) the corresponding spectra of the A and C forms of BEADQ (the images are false-colored based on the chromaticity coordinates determined by the emission spectral response in the 400–720 nm range; scale bar = 50 μm). c) Images recorded using the fluorescence emission in the 400–430 nm window (upper) and optical transmittance (lower), of the A form heated at 70°C for 1–9 min (scale bar = 50 μm).

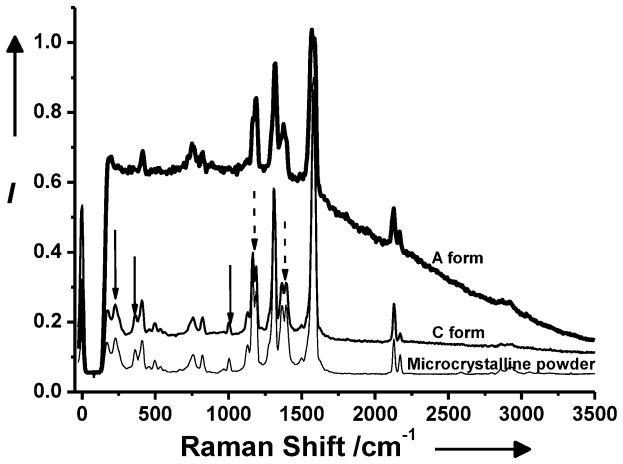

Figure 5. Raman spectra of microcrystalline powder and the C and A forms of BEADQ; peaks present in the microcrystalline powder and C form, but missing (full arrow) or merging (broken arrow) in the A form, are indicated on the spectrum of the C form.

changing between the two phases cannot be ruled out. Even though the origin of the spectral differences requires further investigation, the spectra provide a molecular level signature of the phase change.[31,32]

The significant changes in the fluorescence emission as well as the transmittance of BEADQ between the C and A forms can be exploited in potential applications in information storage; preliminary experiments demonstrate the feasibility of repeated writing and erasing of strongly fluorescent patterns by controlled heating and subsequent melt-quench operations.[26] Aspects like the long term stability of the phases, writing by irradiation to achieve higher resolution and enhancement of switching speeds remain to be addressed. All the alkoxyalkyl chain substituted DADQs we have synthesized show similar PCM behavior and fluorescence switching responses.[26] The relative stability and rates of interconversion are found to vary with the alkoxy group, suggesting that tailoring the molecular structure can lead to optimal materials for unique PCM applications; this highlights the inherent versatility of molecular materials. The family of molecules developed in this study, capable of facile and cyclic phase changes between crystalline and amorphous forms exhibiting prominent fluorescence emission color and intensity switching, form a new class of functional PCMs.

Keywords: amorphous phase · crystalline phase · fluorescence · phase-change materials · supramolecular materials

How to cite: *Angew. Chem. Int. Ed.* **2015**, *54*, 7270–7274
Angew. Chem. **2015**, *127*, 7378–7382

[1] D. C. Hyun, N. S. Levinson, U. Jeong, Y. Xia, *Angew. Chem. Int. Ed.* **2014**, *53*, 3780–3795; *Angew. Chem.* **2014**, *126*, 3854–3871.
[2] K. Pielichowski, K. Pielichowska, *Environ. Prot. Eng.* **2006**, *32*, 203–207.
[3] J.-L. Zeng, F.-R. Zhu, S.-B. Yu, L. Zhu, Z. Cao, L.-X. Sun, G.-R. Deng, W.-P. Yan, L. Zhang, *Sol. Energy Mater. Sol. Cells* **2012**, *105*, 174–178.
[4] K. Tumirah, M. Z. Hussein, Z. Zulkarnain, R. Rafeadah, *Energy* **2014**, *66*, 881–890.
[5] J. Liu, C. Detrembleur, M.-C. De Pauw-Gillet, S. Mornet, L. V. Elst, S. Laurent, C. Jerome, E. Duguet, *J. Mater. Chem.* **2014**, *2*, 59–70.
[6] M.-W. Chang, E. Stride, M. Edirisinghe, *Soft Matter* **2009**, *5*, 5029–5036.
[7] L. F. Cabeza, J. Illa, J. Roca, F. Badia, H. Mehling, S. Hiebler, F. Ziegler, *Mater. Corros.* **2001**, *52*, 140–146.
[8] P. F. Weck, E. Kim, *J. Phys. Chem. C* **2014**, *118*, 4618–4625.
[9] S. Raoux, *Annu. Rev. Mater. Res.* **2009**, *39*, 25–48.
[10] C. E. Giusca, V. Stolojan, J. Sloan, F. Börrnert, H. Shiozawa, K. Sader, M. H. Rümmeli, B. Büchner, S. R. P. Silva, *Nano Lett.* **2013**, *13*, 4020–4027.
[11] C. Rios, P. Hosseini, C. D. Wright, H. Bhaskaran, W. H. P. Pernice, *Adv. Mater.* **2014**, *26*, 1372–1377.
[12] T. P. Radhakrishnan, *Acc. Chem. Res.* **2008**, *41*, 367–376.
[13] Y. Shirota, *J. Mater. Chem.* **2000**, *10*, 1–25.
[14] B. C. Hancock, G. Zografi, *J. Pharm. Sci.* **1997**, *86*, 1–12.
[15] M. Takahashi, N. S. Humam, N. Tsumori, T. Saiki, P. Regreny, M. Gendry, *Appl. Phys. Lett.* **2013**, *102*, 093120.
[16] Y.-J. Jin, B. S.-I. Kim, W.-E. Lee, C.-L. Lee, H. Kim, K.-H. Song, S.-Y. Jang, G. Kwak, *NPG Asia Mater.* **2014**, *6*, e137.
[17] F. Li, J. Zhuang, G. Jiang, H. Tang, A. Xia, L. Jiang, Y. Song, Y. Li, and D. Zhu, *Chem. Mater.* **2008**, *20*, 1194–1196.
[18] D. Yan, J. Lu, J. Ma, M. Wei, D. G. Evans, X. Duan, *Angew. Chem. Int. Ed.* **2011**, *50*, 720–723; *Angew. Chem.* **2011**, *123*, 746–749.
[19] T. Mutai, H. Satou, K. Araki, *Nat. Mater.* **2005**, *4*, 685–687.
[20] X. Luo, J. Li, C. Li, L. Heng, Y. Q. Dong, Z. Liu, Z. Bo, B. Z. Tang, *Adv. Mater.* **2011**, *23*, 3261–3265.
[21] A. H. Sporer, *Appl. Opt.* **1987**, *26*, 1240–1245.
[22] W. R. Hertler, H. D. Hartzler, D. S. Acker, R. E. Benson, *J. Am. Chem. Soc.* **1962**, *84*, 3387–3393.
[23] P. Gangopadhyay, S. Sharma, A. J. Rao, D. N. Rao, S. Cohen, I. Agranat, T. P. Radhakrishnan, *Chem. Mater.* **1999**, *11*, 466–472.
[24] S. Jayanty, T. P. Radhakrishnan, *Chem. Eur. J.* **2004**, *10*, 791–797.
[25] C. G. Chandaluri, T. P. Radhakrishnan, *Angew. Chem. Int. Ed.* **2012**, *51*, 11849–11852; *Angew. Chem.* **2012**, *124*, 12019–12022.
[26] See the Supporting Information.
[27] Crystallographic data: Monoclinic *C*2/*c*, $a = 19.999(9)$, $b = 9.687(4)$, $c = 21.343(9)$ Å, $V = 4132(3)$ Å^3, $\rho_{calc} = 1.146$ g cm^{-3}, $T = 100$ K, no. of measured reflections = 3705, no. of parameters = 347, $R = 0.0594$, $wR^2 = 0.1638$, largest diff. peak, hole = 0.587, −0.047 e Å^{-3}; CCDC 1046619 contains the supplementary crystallographic data for this paper. These data can be obtained free of charge from The Cambridge Crystallographic Data Centre via www.ccdc.cam.ac.uk/data_request/cif.
[28] S. Jayanty, T. P. Radhakrishnan, *Chem. Mater.* **2001**, *13*, 2460–2462.
[29] B. Zalba, J. M. Marín, L. F. Cabeza, H. Mehling, *Appl. Therm. Eng.* **2003**, *23*, 251–283.
[30] K. Rajesh, T. P. Radhakrishnan, *Chem. Eur. J.* **2009**, *15*, 2801–2809.
[31] A. Alkhalil, J. B. Nanubolu, J. C. Burley, *RSC Adv.* **2012**, *2*, 209–216.
[32] F. Zhang, O. Kambara, K. Tominaga, J.-i. Nishizawa, T. Sasaki, H.-W. Wang, M. Hayashi, *RSC Adv.* **2014**, *4*, 269–278.

Received: February 3, 2015
Revised: March 24, 2015
Published online: May 4, 2015

